

## Reflectivity and energy balance in pulsed-laser deposition experiments from mono- and bi-atomic targets

T. Müller,<sup>1</sup> B. K. Sinha,<sup>2</sup> and K. P. Rohr<sup>1</sup><sup>1</sup>*Fachbereich Physik, Universität Kaiserslautern, D-67663 Kaiserslautern, Germany*<sup>2</sup>*Laser & Plasma Technology Division, Bhabha Atomic Research Centre, Mumbai 400 085, India*

(Received 11 December 2001; revised manuscript received 29 March 2002; published 9 August 2002)

Reflectivity and complete energy balance from the planar targets of aluminum, copper, nickel, and molybdenum have been measured using a Nd: glass laser ( $\lambda = 1060$  nm,  $\tau = 5$  ns) in the low intensity regime of laser plasma interaction as a function of focal spot size. The magnitude of partition of total incident laser energy into different channels is observed to decrease as the focal spot size increases. It is further observed that the magnitude of partition of the incident energy into these channels, in general, decreases as the atomic number increases for any given focal spot size, although, the reflectivity component of the partitioned energy increases with focal spot size for any given element. The reflectivities of copper and tungsten and their alloy were measured separately. The reflectivity from the alloy plasma was reduced by a factor of 6 compared to either element separately. This observation confirms the recent theory that in the multiion plasma the ion acoustic waves are additionally damped due to additional Joule, thermal diffusion, and viscous terms in the modified ion-fluid theory of the ion acoustic waves in a multiion species plasma.

DOI: 10.1103/PhysRevE.66.026403

PACS number(s): 52.38.-r, 52.38.Mf, 52.25.Fi, 52.35.Fp

### I. INTRODUCTION

The pulsed-laser deposition (PLD) scheme in the field of material preparation such as fabrication of thin films of high  $T_c$  superconductors, oxides, semiconductors, and diamond-like carbon, has been extensively reported by various workers in the laser intensity regime of  $10^9$  to  $10^{12}$  W/cm<sup>2</sup> [1–13]. These experiments are useful in the investigations of gas dynamics [10,14–16], recombination, and transient thermodynamics [17,18] and the studies of basic physics of laser plasma interaction.

Investigations of partial energy balance and reflectivity have been reported by various workers [19–31], primarily in the nonlinear regime of laser plasma interaction from monoatomic targets. Earlier workers [26,27] reported the measurements of reflectivity from plasmas produced from planar monoatomic targets in the laser intensity regime of  $10^{11}$  to  $5 \times 10^{13}$  W/cm<sup>2</sup>. The laser intensity was varied either by keeping the focal spot diameter constant and varying the energy or by keeping the laser energy constant and varying the focal spot diameter. They observed the variation of total reflectivity in the range of 5 to 35 % and noted that the light absorption did not depend on the laser intensity alone but was also affected by the irradiated focal spot diameter. Lahiri and Sinha [29,30] and Gupta and Sinha [31] investigated the reflectivity of a phase conjugate wave via four-wave mixing in a laser produced plasma at an intensity of about  $5 \times 10^{13}$  W/cm<sup>2</sup> and reported that ion acoustic waves (IAW) have an important role to play. Bychenkov, Rozmus, and Tikhonchuk [28] reported on stimulated Brillouin scattering (SBS) reflectivity from a plasma composed of two ion species. Their analysis has demonstrated a very sensitive dependence of the IAW damping rate on the plasma-ion composition. They observed that the SBS reflectivity from a C<sub>5</sub>H<sub>12</sub> target is approximately five to ten times lower than that from a C<sub>5</sub>D<sub>12</sub> plasma with the same plasma parameters because

damping of ion acoustic waves in a C<sub>5</sub>D<sub>12</sub> plasma is much smaller than that in a C<sub>5</sub>H<sub>12</sub> plasma. They further noted that the charge-to-mass ratio, i.e.,  $Z/M$ , has a significant role to play in additional damping due to the friction force.

The efficiency of energy coupling to the plasma and the partition of the laser energy into different channels play an important role in the understanding of theoretical as well as practical applications of laser ablation. For the PLD process, knowledge of the integrated kinetic energy of the plasma particles that strike the substrate and, in general, the complete energy balance is very important because the properties and the quality of the deposited layers are substantially influenced by them [32].

In the present work we present a complete measurement of the total energy balance from laser produced aluminum, copper, nickel, and molybdenum plasma hitherto unreported in any intensity regime of laser plasma interaction. We have measured the fraction of laser energy going into different channels with an accuracy varying from  $\pm 10$  to  $\pm 15$  % and present a justification for ignoring the energy going into other channels like heat conduction, collision, emission, and magnetic field. Moreover, we have measured the reflectivities of tungsten and copper and their alloy W<sub>34</sub>Cu<sub>66</sub> within an error margin of 15%. Measurements confirm the decrease in reflectivity from the alloy based on the theory of the damping of ion acoustic waves [28,33,34].

### II. EXPERIMENTAL AND THEORETICAL CONSIDERATION

The investigations of energy balance and reflectivity were carried out for laser produced plasmas generated from slab targets of aluminum, copper, nickel, molybdenum, tantalum, and tungsten. An alloy of tungsten and copper (W<sub>34</sub>Cu<sub>66</sub>) was also considered. The laser beam ( $\lambda = 1060$  nm,  $\tau = 5$  ns) was incident at an angle of 45° with respect to the target surface. The laser spot size was varied between 0.61

and  $8.34 \text{ mm}^2$  at a constant laser pulse energy of 130 mJ by moving the focussing lens up and down from a fixed position. The resulting laser intensity variation, in the range of  $3.1 \times 10^8$  to  $4.3 \times 10^9 \text{ W/cm}^2$ , was suitable for PLD experiments. As the hydrodynamics of plasma expansion is greatly affected by the area of expansion, or focal spot size [35–37], all the experimental results have been displayed as a function of the focal spot diameter at a fixed laser energy. The experiments were carried out inside a vacuum chamber with a background pressure of  $p < 10^{-6}$  mm of Hg. In the case of the W-Cu alloy, the smallest ablation area was chosen to be about an order of magnitude larger than the size of granulation in the alloy, about 0.44 mm in diameter. The targets were supplied by Good Fellow Cambridge Limited, UK and all of them had a surface uniformity of better than  $5 \mu\text{m}$ . The surface uniformity was ascertained with the help of a roughness monitor (Perthometer) C5D supplied by the firm Mahr (Perthen), Germany. The particles of the freely expanding plasma were detected in an angular range relative to the target normal, between  $\phi_{\text{RPA}} = 50^\circ$  to  $10^\circ$  for ions and  $\phi_Q = 80^\circ$  to  $-15^\circ$  for the total number of particles, by moving around the analyzers within the plane of incidence. The analyzers were located at a distance of 35 cm from the target. The ion spectra were fully resolved by the time of flight/retarding potential method, which made it possible to obtain the absolute number of each ion species. Up to four times charged ions were recorded. The second detector essentially consisted of an rf-excited quartz crystal. After the plasma had been deposited onto the crystal, the frequency change of the crystal gave the total mass or, in the case of monoatomic beams, the total number of particles. The error budget for the measurements included careful determination of the laser parameters, transmission function of the ion-detector, linearity of the frequency response, sticking efficiency, the temperature effects of the crystal, surface finish of the different targets, and size and geometry of the ablation area. Details of the experimental arrangement as well as measurement and

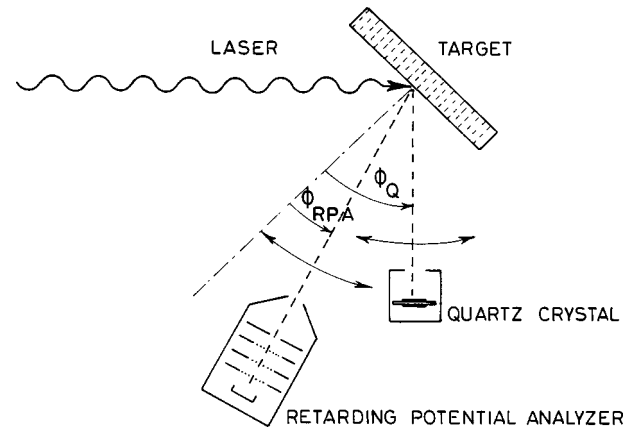


FIG. 1. A schematic diagram of the experimental setup.

control procedures have been described in the earlier publications [18,38,39]. A schematic diagram is shown in Fig. 1.

The energy of the reflected laser light was measured with a calibrated energy meter (RJP700, Laser Precision Corporation, USA). For protection against the flying plasma particles and for the sake of wavelength selection an IR filter ( $\lambda = 1064 \text{ nm}$ ,  $\Delta\lambda = 8.7 \text{ nm}$  full width at half maximum) was mounted before the measuring head. The energy meter could be turned around in the angular range of  $-20^\circ$  to  $+90^\circ$  with respect to the target normal. The portion of the laser light which was back reflected in the direction of the incident laser light was neglected. Spot-checks of out-of-plane emission were made to ensure that it likewise could be neglected. The reflected laser energy was taken to be the sum of the individual contributions of the reflected energies from each investigated direction in the aforesaid angular range. The main reflection direction was found to be in the direction of geometrical reflection ( $\phi_Q = 45^\circ$ ) in all investigations.

The energy balance in the present experiment consisted of the following:

$$E_{\text{Laser}} = E_{\text{Reflection}} + E_{\text{Fusion}} + E_{\text{Vaporization}} + E_{\text{Ionization}} + E_{\text{kin.Ion}} + E_{\text{kin.Atom}} + E_{\text{Other channels}}, \quad (1)$$

$$E_{\text{Other channels}} = E_{\text{Heat conduction}} + E_{\text{Collision}} + E_{\text{Emission}} + E_{\text{Magnetic field}}, \quad (2)$$

where  $E_{\text{Laser}}$  is the incident laser energy,  $E_{\text{Reflection}}$  is the reflected light from target surface and plasma,  $E_{\text{Fusion}}$  is the fusion energy,  $E_{\text{Vaporization}}$  is the vaporization energy,  $E_{\text{Ionization}}$  is the ionization energy,  $E_{\text{kin.Ion}}$  is the kinetic energy of ions,  $E_{\text{kin.Atoms}}$  is the kinetic energy of neutral atoms,  $E_{\text{Collision}}$  is the energy loss through collision,  $E_{\text{Emission}}$  is the radiation loss through bremsstrahlung, recombination, and line emission, and  $E_{\text{Magnetic field}}$  is the energy loss through magnetic field.  $E_{\text{Reflection}}$  can be obtained by infrared measurements using the energy meter described in the preceding paragraph. The fusion and vaporization energies  $E_f$  and  $E_v$  can be obtained from the measurement of the absolute total

number of particles  $N_{\text{int}}^{\text{tot}}$  and from molar heat and vaporization energies  $\Delta H_f$  and  $\Delta H_v$ , respectively, from the equation given below,

$$E_{f,v}(\text{mJ}) = \frac{N_{\text{int}}^{\text{tot}}}{6.02 \times 10^{23} (\text{mol}^{-1})} \Delta H_{f,v} (\text{mJ/mol}). \quad (3)$$

The ionization energy follows from  $q$  times the number of ionized ions  $N_{\text{int}}^{q+}$  and the molar ionization energy  $\chi^i$  for the charge state  $i$  as follows:

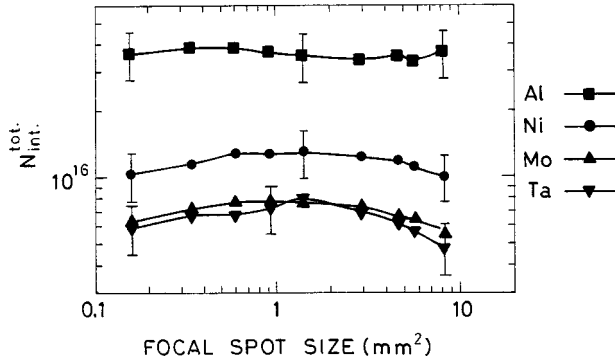


FIG. 2. Total number of angular integrated particles  $N_{\text{int}}^{\text{tot}}$  as a function of focal spot size for Al, Ni, Mo, and Ta.

$$E_{\text{ionization}}(\text{mJ}) = \sum_{q=1}^{q_{\text{max}}} \left( \sum_{i=1}^q \chi^i (\text{mJ/mol}) \right) N_{\text{int}}^{q+} / 6.02 \times 10^{23} (\text{mol}^{-1}). \quad (4)$$

The specific heats and the ionization energies were obtained from the works of Emsley [40]. The sum of the kinetic energies of all the ions is given by summing over the total kinetic energy  $E_{\text{tot}}^{q+}$  of ions of charge state  $q+$ , given by the equation

$$E_{\text{kin.ion}} = \sum_i^q i E_{\text{tot}}^{q+} = \sum \int \frac{dE_{\text{tot}}^{q+}}{d\Omega}(\theta) d\Omega = 2\pi \sum \int_0^{\theta_{\text{max}}} \frac{dE_{\text{tot}}^{q+}}{d\Omega}(\theta) \sin(\theta) d\theta, \quad (5)$$

where  $\theta$  is the direction with respect to the target normal. Measurement of the kinetic energies of the neutral atoms and the distribution of energy into other channels [Eq. (1)] was not performed in this experiment. Therefore, the kinetic energies of the neutral atoms cannot be deduced accurately. However, the upper limits have been presented using Eq. (1).

III. RESULTS AND DISCUSSION

Figure 2 shows the variation in the total number of integrated particles  $N_{\text{int}}^{\text{tot}}$  as a function of the focal spot size, at an incident laser energy of  $E_{\text{Laser}} = 130$  mJ, for the different materials Al, Ni, Mo, and Ta. The number of particles varies between  $4.75 \times 10^{15}$  and  $3.87 \times 10^{16}$  and decreases with increasing atomic number. The reason for this decrease lies in complex interaction of the various material properties such as reflectivity, thermal diffusion length, and vaporization

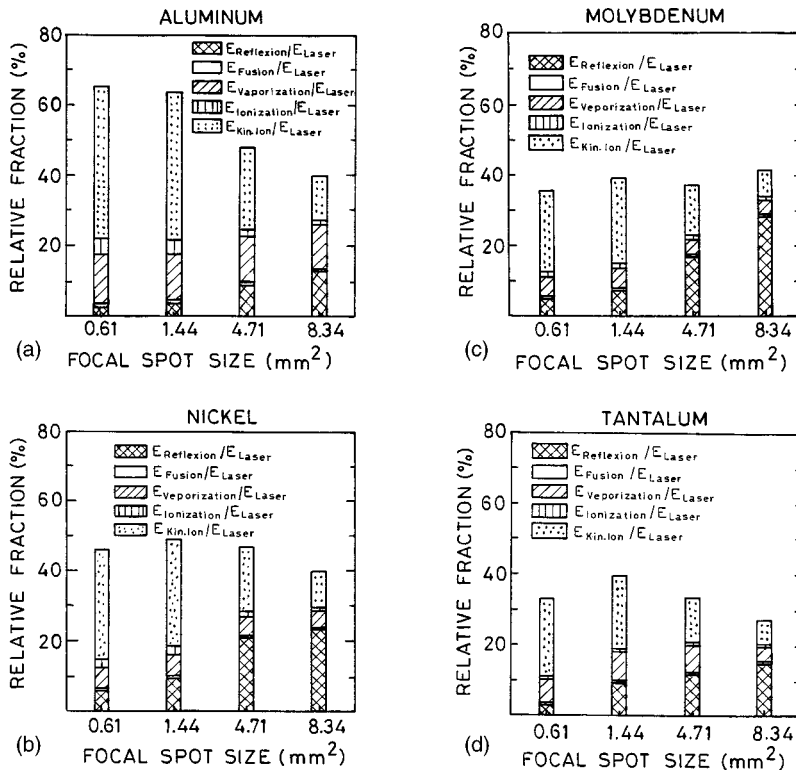


FIG. 3. (a)–(d) Energy balance for different target materials as a function of focal spot size for an incident laser energy of 130 mJ. Relative fraction is with reference to laser energy.

TABLE I. Integrated kinetic energies (mJ) of each ionization state as a function of focal spot size  $B$ . The data for the neutral atoms are as per Eq. (6) and represent the upper limit for a laser energy of  $E_{\text{Laser}} = 130$  mJ.

$B$ (mm <sup>2</sup> )	Ionization state	Aluminum	Nickel	Molybdenum	Tantalum
0.61	0	<45.2	<69.8	<83.9	<86.8
	1	7.0	9.8	11.4	16.0
	2	23.1	16.1	10.3	7.5
	3	20.7	9.0	5.0	3.0
	4	5.3	5.9	3.5	2.2
1.44	0	<47.3	<66.6	<79.5	<79.0
	1	11.5	13.3	14.4	17.3
	2	26.0	16.0	10.3	5.9
	3	13.9	7.0	6.4	2.1
	4	2.6	3.2		1.4
4.71	0	<67.9	<69.2	<82.3	<87.1
	1	14.3	12.3	10.3	11.7
	2	14.3	9.3	10.4	3.5
	3	1.8	2.4	3.0	0.94
	4				
8.34	0	<78.3	<78.1	<77.3	<95.5
	1	10.6	9.1	6.1	6.9
	2	5.3	4.0	3.0	1.8
	3	0.5	0.6	1.1	0.6

energy, which give a limit to the ablation threshold of the individual target materials as reported by Rubahn [41]. The integrated particle number shows little dependence on the focal spot size and may be approximated as being constant over the complete regime of the focal spot size. This means that the number of the ablated particles in the presently investigated range of focal intensity is determined only by the pulse energy and not by the pulse intensity. This implies that the laser-target interaction is dominated by linear absorption, and that all nonlinear processes may be ignored in Eq. (1). The number of ablated particles has been used to calculate the fusion and vaporization energies from Eq. (3).

In Figs. 3(a)–3(d) the relative share of the measured energy going into five different energy channels denoted in Eq. (1), for a laser energy of 130 mJ, and its dependence on the laser spot size ( $B$ ) have been displayed for the target materials Al, Ni, Mo, and Ta. These energy channels have a share of the total incident energy varying from 26% (tantalum,  $B = 8.34$  mm<sup>2</sup>) to 64% (aluminum,  $B = 0.61$  mm<sup>2</sup>). All the target materials jointly show that the reflectivity increases with increasing focal spot size ( $B$ ), by a factor of 3.9 for nickel and 5.7 for molybdenum. For the same variation in  $B$ , the kinetic energy of ions varies relatively strongly between a factor of 2.9 (aluminum) and a factor of 3.1 (tantalum), whereas the residual energies vary relatively weakly between a factor of 1.3 (aluminum) and 1.6 (tantalum).

It is to be noted that for all the samples the reflectivity increases as the focal spot size increases. This is because the plasma front appears more like a smooth, plane mirror to the incident laser light for  $B = 8.34$  mm<sup>2</sup> than for the focal spot sizes of decreasing dimensions. With the decreasing focal spot size, the curvature of the plasma front increases. As a

result, the reflectivity decreases and the incident laser light is better coupled to the plasma [26,27]. A smaller laser-spot size on the target surface produces larger density gradients and the plasma expansion is less of a one-dimensional character, resulting in the availability of smaller interaction length for Brillouin scattering in the underdense plasma, and, hence, the reflectivity decreases. Spot checks for out-of-plane emission gave negligible results. In general, Figs. 3(a)–3(d) show that the magnitude of the total incident energy transferred into these five different channels decreases as the atomic number of the target material increases, within the limits of experimental errors, estimated to be under 10%.

We have considered the upper limit of the kinetic energy of neutral atoms  $E_{\text{kin.Atoms}}^{\text{max}}$  ignoring the partition of energy into other channels as defined in Eq. (2) as per the equation given below,

$$E_{\text{kin.Atoms}}^{\text{max}} = E_{\text{Laser}} - (E_{\text{Reflection}} + E_{\text{Fusion}} + E_{\text{Vaporization}} + E_{\text{Ionization}} + E_{\text{kin.Ion}}). \quad (6)$$

These values, together with the integrated kinetic energy  $E_{\text{tot}}^{\text{q}+}$  of the individual ions have been displayed in Table I for an incident laser energy of 130 mJ. It is to be noted that the integrated kinetic energy of ions, according to Eq. (5), depends both on the velocity and the absolute number of particles. It is seen that when we add up the kinetic energies of the neutral atoms and the ions of each ionization state and consider the reflectivity as displayed in Table II for any chosen focal spot size, the total energy comes reasonably close to the incident laser energy of 130 mJ. For example, in the case of Al, Fig. 3(a) gives the fraction of laser energy going

TABLE II. Measured reflectivity (%) above the plasma production threshold for a laser energy of  $E_{\text{Laser}} = 130$  mJ.  $B$  is the focal spot size.

Material	$B = 0.61 \text{ mm}^2$	$B = 1.44 \text{ mm}^2$	$B = 1.74 \text{ mm}^2$	$B = 4.71 \text{ mm}^2$	$B = 8.34 \text{ mm}^2$
Aluminum	$2.7 \pm 0.6$	$3.9 \pm 0.9$		$8.9 \pm 1.4$	$12.9 \pm 4.1$
Nickel	$6.0 \pm 2.2$	$9.5 \pm 2.9$		$20.8 \pm 3.6$	$23.2 \pm 3.8$
Molybdenum	$4.9 \pm 1.2$	$7.2 \pm 2.5$		$16.3 \pm 3.5$	$27.8 \pm 7.2$
Tantalum	$2.8 \pm 0.7$	$8.9 \pm 0.9$		$11.4 \pm 2.5$	$14.3 \pm 4$
Tungsten			$15.7 \pm 3.3$		
Copper			$14.4 \pm 2.9$		
$\text{W}_{34}\text{Cu}_{66}$			$2.5 \pm 0.4$		

into different channels, excluding the other channels defined in Eq. (2) and the kinetic energies of the neutral atoms, for  $B = 0.61, 1.44, 4.71,$  and  $8.34 \text{ mm}^2$  as 66, 63, 43, and 40%, respectively, which come out to be 85.8, 81.9, 59.8, and 52.0 mJ. From Table I, for these values of  $B$ , estimated upper limits of the kinetic energies of the neutral atoms are 45.2, 47.3, 67.9, and 78.3 mJ. Summing up, we get the total energies as 131.0, 129.2, 127.7, and 130.3 mJ. Similarly, we can get the results for other elements.

In Fig. 4 the integrated average ion energy,  $E_{\text{kin.Ion}}$  and the maximum average energy of the neutral atoms,  $\bar{E}_{\text{kin.Atom}}^{\text{max}}$ , are displayed as a function of the focal spot size. It is to be noted that  $\bar{E}_{\text{kin.Atom}}^{\text{max}}$  is smaller than  $E_{\text{kin.Ion}}$  for all the target materials. This is important because the kinetic energies of the ablated neutral particles have never been measured earlier in the asymptotic range. This paper gives quantitative upper limits for the velocities of neutral particles. Moreover, for the adoption of plasma models and simulation of plasma expansion dynamics, it is important to know the absolute energy content of the neutral particles [9], where it is generally assumed that the neutral particles are slower than singly charged ions. With increasing focal spot size the average kinetic energy of ions decreases by a factor of 3 [aluminum:  $E_{\text{kin.Ion}}(B = 0.61 \text{ mm}^2) = 302 \text{ eV}$ ,  $E_{\text{kin.Ion}}(B = 8.34 \text{ mm}^2) = 105 \text{ eV}$ ]. For each focal size, the average ionic kinetic en-

ergy varies little with atomic number (only 11%), although the difference in the ion energy increases with increasing focal spot size.

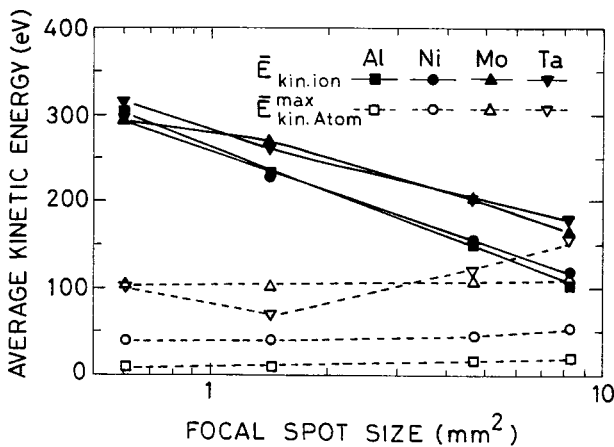
Table III displays the reflectivity from various targets below the plasma production threshold ( $E_{\text{Laser}} = 0.22$  mJ). The reflectivity was found to be independent of the focal spot size. Table II shows the reflectivity above the plasma threshold and is found to be dependent on the focal spot size. For each target material the reflectivity increases with the increase in focal spot size as explained in the preceding paragraph.

Earlier workers [29–31] have reported a significant role for IAW with reference to phase conjugate reflectivity of the laser produced plasma. The works of Turner *et al.* [33], Epperlein, Short, and Simon [34], and Bychenkov, Rozmus, and Tikhonchuk [28] are significant in this connection. Turner *et al.* reported experiments on nova and presented Brillouin scattering measurements obtained from cylindrical (2.5 mm diameter and 2.5 mm long) gas filled haulraums which contained 1 atm of neoprene gas. Their data show that while large levels of SBS can be generated under some conditions, the instability is reduced to low levels for conditions in which IAW are considerably damped for multiion species, depending on their  $Z/M$  ratios.

Bychenkov, Rozmus, and Tikhonchuk [28], in their theoretical formulation, observed that the SBS reflectivity depends strongly on the ion composition. They reported that the SBS reflectivity from a  $\text{C}_5\text{H}_{12}$  target is approximately five to ten times lower than that from a  $\text{C}_5\text{D}_{12}$  plasma with the same parameters. They related this observation to the composition-dependent damping of the ion acoustic waves.

 TABLE III. Measured reflectivity below the plasma production threshold of  $E_{\text{Laser}} = 0.22$  mJ. The reflectivity does not depend on the focal spot size.

Material	Reflectivity (%)
Aluminum	$58.3 \pm 2.4$
Nickel	$46.0 \pm 1.6$
Molybdenum	$44.7 \pm 1.6$
Tantalum	$62.8 \pm 1.7$
Tungsten	$46.3 \pm 0.5$
Copper	$60.1 \pm 0.6$
$\text{W}_{34}\text{Cu}_{66}$	$12.3 \pm 0.5$


 FIG. 4. Integrated average ion-kinetic energy  $\bar{E}_{\text{kin.Ion}}$  and upper limit  $\bar{E}_{\text{kin.Atom}}^{\text{max}}$  of the average kinetic energy of neutral atoms as a function of focal spot size ( $E_{\text{Laser}} = 130$  mJ).

The major difference between a  $C_5H_{12}$  and a  $C_5D_{12}$  plasma is that the charge-to-mass ratio, i.e.,  $Z/M$  is  $\frac{1}{2}$  for  $C^{6+}$  and 1 for  $H^+$ , while  $Z/M$  is  $\frac{1}{2}$  for  $D^+$ . Therefore, in a  $C_5H_{12}$  plasma, the ion acoustic wave exhibits an additional damping related to the friction forces. They attributed the lower scattering from a  $C_5H_{12}$  plasma to a higher damping rate of IAW than that which occurs in  $C_5D_{12}$ . Epprelein, Short, and Simon [34] calculated the collisional damping of ion acoustic waves for a mixture of light and heavy ions and modified the frequently used single-species average ion model. They considered the effects of a new Joule term, thermal diffusion, and viscous damping terms, which affect the damping of ion acoustic waves.

In Table II we can observe the reflectivities from tungsten, copper, and an alloy of W and Cu in the stoichiometric proportion of  $W_{34}Cu_{66}$ . For a focal spot size of  $B=1.74\text{ mm}^2$  the reflectivities from tungsten and copper were measured to be  $15.7\pm 3.3\%$  and  $14.4\pm 2.9\%$ , respectively, that is, they individually showed nearly equal reflectivity. However, the

alloy  $W_{34}Cu_{66}$  showed a reflectivity of only  $2.5\pm 0.4\%$ . In the case of the alloy, which is a mixture of the two elements, reflectivity showed a decrease by a factor of nearly 6. From the works of Bychenkov, Rozmus, and Tikhonchuk and Epprelein, Short, and Simon we conclude that in the case of  $W_{34}Cu_{66}$  additional damping of ion acoustic waves takes place due to new Joule, thermal diffusion, and viscous damping terms, which are absent in the case of single species W and Cu plasma. As a result, the reflectivity is reduced due to the relatively low magnitude of the ion acoustic waves. Our results for  $W_{34}Cu_{66}$  seem to support these models.

#### ACKNOWLEDGMENTS

The authors gratefully acknowledge the technical assistance of Hans Jürgen Feurich. One of us (B.K.S.) is very thankful to the Alexander Von Humboldt Foundation for financial support.

- 
- [1] R. K. Singh and J. Narayan, *Phys. Rev. B* **41**, 8843 (1990).  
 [2] D. K. Fork, J. B. Joyce, F. A. Ponee, R. I. Johnson, G. B. Anderson, G. A. N. Connell, C. B. Eom, and T. H. Geballe, *Appl. Phys. Lett.* **53**, 337 (1988).  
 [3] D. Sibold and H. M. Urbassek, *Phys. Rev. A* **43**, 6722 (1991).  
 [4] K. Mann and K. Rohr, *Laser Part. Beams* **10**, 435 (1992).  
 [5] Roger Kelly, *Phys. Rev. A* **46**, 860 (1992).  
 [6] R. Kelly, A. Miotello, B. Braven, A. Gupta, and K. Casey, *Nucl. Instrum. Methods Phys. Res. B* **65**, 187 (1992).  
 [7] D. Sibold and H. M. Urbassek, *J. Appl. Phys.* **73**, 8544 (1993).  
 [8] A. Thum, A. Rupp, and K. Rohr, *J. Phys. D* **27**, 1791 (1994).  
 [9] G. Granse, S. Völlmar, A. Lenk, A. Rupp, and K. Rohr, *Appl. Surf. Sci.* **96**, 97 (1996).  
 [10] S. I. Anisimov, D. Bäuerle, and B. S. Luk'yanchuk, *Phys. Rev. B* **48**, 12 076 (1993).  
 [11] R. Kelly and A. Miotello, *Nucl. Instrum. Methods Phys. Res. B* **91**, 682 (1994).  
 [12] E. Buttini, A. Thum-Jäger, and K. Rohr, *J. Phys. D* **31**, 2165 (1998).  
 [13] M. Tyunina and S. Leppovuori, *J. Appl. Phys.* **87**, 8132 (2000).  
 [14] I. V. Nemchinov, *J. Appl. Math. Mech.* **29**, 143 (1965).  
 [15] F. J. Dyson, *J. Math. Mech.* **18**, 91 (1968).  
 [16] S. I. Anisimov and Iu. I. Lysikov, *J. Appl. Math. Mech.* **34**, 882 (1970).  
 [17] A. Thum-Jäger, B. K. Sinha, and K. P. Rohr, *Phys. Rev. E* **61**, 3063 (2000).  
 [18] A. Thum-Jäger, B. K. Sinha, and K. P. Rohr, *Phys. Rev. E* **63**, 061405 (2001).  
 [19] F. Floux, J. F. Benard, D. Congnard, and A. Saleres, in *Laser Interactions and Related Plasma Phenomena*, edited by H. Schwartz and H. Hora (Plenum Press, New York, 1972), Vol. 2, p. 409.  
 [20] K. Eidmann and R. Sigel, in *Laser Interaction and Related Plasma Phenomena*, edited by H. Schwartz and H. Hora (Plenum Press, New York, 1973), Vol. 3, p. 667.  
 [21] P. E. Dyer, D. J. James, S. A. James, and M. A. Skipper, *Phys. Lett.* **48A**, 311 (1974).  
 [22] C. Yamanaka, M. Yakoyama, S. Nakai, T. Sasaki, K. Yoshida, M. Matoba, C. Yamabe, T. Tschudi, T. Yamanaka, J. Mijui, N. Yamaguchi, and K. Nishikawa, in *Proceedings of the 7th International Conference on Plasma Physics and Controlled Nuclear Fusion Research, Innsbruck* (IAEA, Vienna, 1979), Vol. 3, p. 421.  
 [23] N. G. Basov, A. R. Zaritskii, S. Zakharov, O. N. Krokhin, P. G. Krynkov, Yu. A. Matveets, Yu. V. Senaskii, and A. I. Fedmisov, *Sov. J. Quantum Electron.* **2**, 439 (1973).  
 [24] J. N. Olson, E. D. Jones, and C. W. Gobeli, *J. Appl. Phys.* **43**, 3991 (1972).  
 [25] A. Carion, J. Lancelot, J. DeMetz, and A. Saleres, *Phys. Lett.* **45A**, 439 (1973).  
 [26] R. D. Godwin, C. G. M. Van Kessel, J. N. Olson, P. Sachsenmaier, R. Sigel, and K. Eidmann, *Z. Naturforsch. A* **32A**, 1100 (1977).  
 [27] H. C. Pant, S. Sharma, T. P. S. Nathan, and T. Desai, *Appl. Phys.* **23**, 183 (1980).  
 [28] V. Yu. Bychenkov, W. Rozmus, and V. T. Tikhonchuk, *Phys. Rev. E* **51**, 1400 (1995).  
 [29] J. Lahiri and B. K. Sinha, *Opt. Commun.* **113**, 407 (1995).  
 [30] J. Lahiri and B. K. Sinha, *Phys. Plasmas* **2**, 1696 (1995).  
 [31] G. P. Gupta and B. K. Sinha, *Phys. Plasmas* **3**, 3614 (1996).  
 [32] D. H. Lowendes, D. B. Geohegan, A. A. Poretzky, D. P. Norton, and C. M. Roulean, *Surf. Sci.* **273**, 898 (1996).  
 [33] R. E. Turner, C. A. Back, R. L. Berger, R. L. Kaufmann, D. H. Kalantar, D. E. Klem, B. F. Lasinski, B. J. MacGowan, D. S. Montgomery, L. V. Powers, T. D. Shepard, and G. F. Stone, *Bull. Am. Phys. Soc.* **39**, 1662 (1994).  
 [34] E. M. Epperlein, R. W. Short, and A. Simon, *Phys. Rev. E* **49**, 2480 (1994).  
 [35] M. J. Herbst, J. Grun, J. Gardner, J. A. Stamper, F. C. Young, S. P. Oberchain, E. A. McLean, and B. H. Ripin, *Phys. Rev. Lett.* **52**, 192 (1984).  
 [36] A. Ng, P. Celliers, D. Pasini, J. Kwan, D. Parfenink, and L. Da

- Silva, Phys. Fluids **27**, 2774 (1984).
- [37] K. Estabrook, Phys. Fluids **29**, 3093 (1986).
- [38] A. Thum-Jäger and K. Rohr, J. Phys. D **32**, 2827 (1999).
- [39] Th. Müller and Klaus Rohr, J. Phys. D **35**, 1 (2002).
- [40] J. Emsley, *The Elements* (Clarendon Press, Oxford, 1989).
- [41] H. G. Rubahn, *Laseranwendungen in der Oberflächen Physik und Materialbearbeitung* (Teubner Studienbücher, B. G. Teubner, Stuttgart, 1996).